doi:10.1017/S1431927615013203

Towards a High-Brightness Electron Impact Ion Source for Nano-Applications

Olivier De Castro[1], David Dowsett[1], Tom Wirtz[1] and Serge Della Negra[2]

[1.] Department "Science and Analysis of Materials" (SAM), Centre de Recherche Public – Gabriel Lippmann, Belvaux, Luxembourg.
[2.] Institut de Physique Nucléaire Orsay (IPNO), Université Paris Sud, Orsay, France.

Introduction

A vast number of nano-scale techniques are based on a finely Focused Ion Beams (FIB) [1]. FIB instruments are used for nano-fabrication techniques such as milling, ion-induced deposition or etching [2]. For Transmission Electron Microscopy a FIB can be used as a sample preparation tool [3]. Moreover, FIB columns are used for imaging purposes on the nano-scale. The Helium Ion Microscope (HIM) for example uses a He^+ beam to perform high-resolution microscopy [4]. Analytical applications such as Secondary Ion Mass Spectrometry (SIMS) use a FIB as primary ion beam (e.g. Cs^+, O_2^+, O^-) to sputter the specimen and create localised ion emission (secondary ions) characteristic for each specimen [5]. All of these FIB nano-applications need high brightness ion sources in order to combine a finely focused ion beam (high lateral resolution) with a sufficiently high beam current (reasonable erosion rates, large secondary electron/ion yields). Additionally, an ion beam with a small energy spread (ΔE) will be favourable to significantly limit the chromatic aberrations within the ion column. Different gas ion sources (e.g. plasma/laser-ionization/electron impact/gas field ion sources) have been designed to develop a high brightness, robust and small ΔE ion source, offering flexibility in the ion species choice [6]. However, so far none of these designs was able to combine all of these desired performances. For some achieving a stable operation represents a difficult task and they still provide an ion beam with an energy spread of a few eV. The atomic level ion source used in the HIM is capable of producing a very high brightness low ΔE ion beam but the available ion species are limited to Helium and Neon. For most of these sources the technical requirements are complex resulting in a large physical size. Therefore, it is desirable to design an ion source combining a small physical size, a reduced complexity of the technical requirements, a broad range of ion species with a high brightness low ΔE ion beam. This would give the source the capability of being used as a compact versatile add-on tool for FIB-applications.

This paper concentrates on the concept of an electron impact (EI) ion source. The technical requirements of the planned source are kept reasonably basic as it can be operated at room temperature and the optical design will be fully electrostatic. Furthermore, a flexible ion species range can be realised by essentially only changing the gas feed. Conventional EI-ion sources are very often based on the design proposed by Nier [7] in which an electron beam emitted by a heated filament is guided into an ionization cell, see Figure 1a. In this design, the ions are extracted from a cubic mm sized ionization volume (IV). Reducing the IV to the micron scale leads to a reduced virtual source size of the ion beam and an increased brightness should be achievable [8]. In our design an electron column is used to focus the beam to the µm range above an ion extraction aperture with a diameter d_{Extr} in the order of 100 µm or less. This leads to the desired IV of micron scale. The ionization cell will essentially be composed of two parallel plates of sub-millimeter spacing d_{Plates}, see Figure 1b. The ion beam energy spread ΔE is mainly related to the applied potential difference ΔV_{Plates}. The ions leave from different equipotential surfaces parallel to the plates' surfaces. Applying only a few volts of ΔV_{Plates} leads to a small potential difference between adjacent equipotential surfaces. The combination of a micron scale ionization volume and a small potential difference across the ionization volume leads to an energy spread ΔE < 1 eV. In the following,

charged particle optics (CPO) simulations and methodologies which were used to determine the achievable ion source brightness will be discussed in more detail.

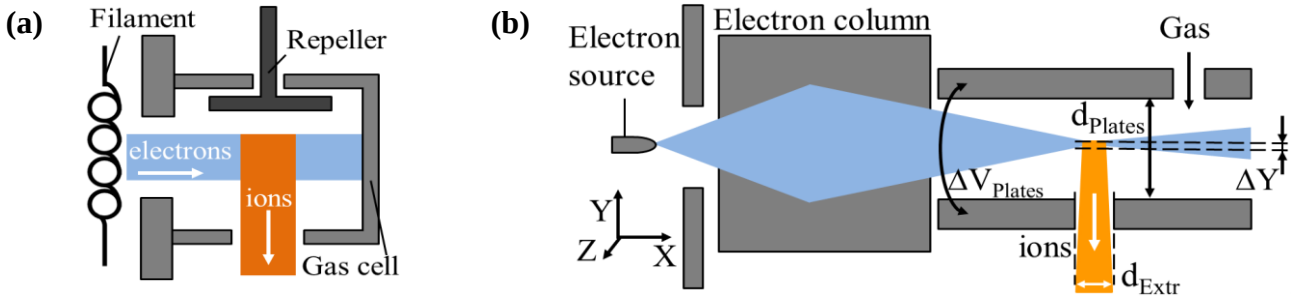

Figure 1. Schematics: (a) Nier type based EI-ion source; (b) Intended design for the new EI-ion source.

Design of a small electron column

The first investigations considered the design of a small electron column (length × diameter ≈ 60 × 20 mm) in order to focus the electron beam inside the ionization cell. All CPO-simulations have been performed with SIMION [9]. The electron column was composed of several components, see Figure 2: a triode extraction region; a first parallelising lens; a set of deflectors and a second focusing lens. A fixed voltage difference of 5 kV was applied between Wehnelt and anode. In order to limit the effective emission area to the front part of the filament tip a bias-voltage of -75 V was applied between Wehnelt and filament. Both lenses were operated in decelerating mode. The column was modelled using multiple boundary matched potential arrays (PA). This technique [10] allows PAs with high and low density meshes to be overlapped while avoiding unrealistic discontinuities in potential to ensure maximum accuracy of the simulations. To simulate the electron emission from the filament Monte-Carlo techniques were used to generate random but uniformly distributed emission locations on the filament tip surface. The electrons were emitted randomly in all directions from a hairpin filament of a diameter $d_{Filament}$ = 0.13 mm. As an approximation an initial Maxwell-Boltzmann kinetic energy distribution corresponding to the applied filament temperature has been used. To estimate the emitted electron current, the following formula was used:

$$I_{Electron} = A_{Emission}\, j_{Thermionic}\, f_{Extraction} \qquad (1).$$

Where $A_{Emission}$ is the emission area of all extracted electrons and can be approximated for the hairpin filament as the half-surface area of a tri-axial ellipsoid. $j_{Thermionic}$ represents the thermionic emission current density: $j_{Thermionic} \sim T^2 \exp(-\Phi/(k_B T))$. T is the filament temperature (set to 2700 K), Φ the work function (set to 4.5 eV for a tungsten filament) and k_B is the Boltzmann-constant [11]. A factor $f_{Extraction}$ needs to be taken into account as only a certain amount of all electrons emitted within $A_{Emission}$ pass through the extraction aperture. The second important quantity to determine the performance of the electron column is the achievable beam focus above the ion extraction aperture. For this purpose the electrons' positions and velocities are recorded at an YZ-cross plane within a field free region inside the ionization cell, see Figure 2. Trajectory extrapolation (electron paths are straight in a field free region) was used in positive X-direction in order to determine the size variation of the disc containing 50% of the total beam current (FW50), Figure 3a. The beam focus was defined as the minimal FW50. This procedure was used to determine the achievable spot size for several final beam energies in the range 0.1 to 1 keV, covering the relevant energy range for the EI-process. The results are shown in Figure 3b. The FW50 current shows a slight variation over the energy range.

https://doi.org/10.1017/S1431927615013203 Published online by Cambridge University Press

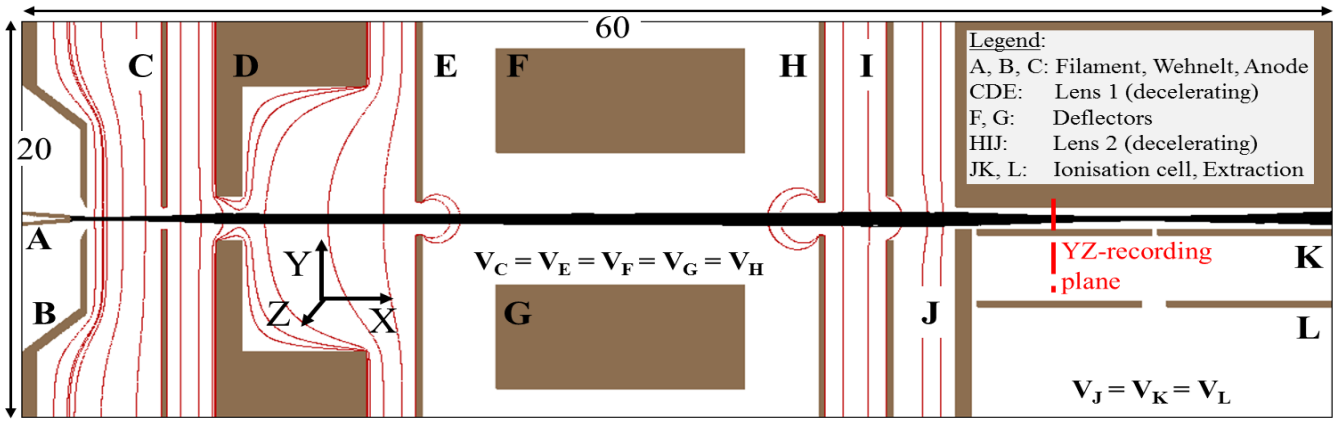

Figure 2. CPO-simulation of the electron column; Filament (d = 0.13 mm, T = 2700 K, Φ = 4.5 eV); Final beam energy 1 keV; V_A = 4 kV, V_C = 9 kV, ΔV_{BC} = -75 V and V_J = 5 kV; dimensions in mm.

As the extraction conditions are independent of the final beam energy the variation is related to the statistical variation of $A_{Emission}$ and to the total number of electrons generated within this area. Taking the weighted mean value over the energy range leads to $I_{Electron\_FW50}$ = 40 µA. The electron beam focus decreases from 190 µm at 100 eV to approximately 95 µm at 1 keV (a factor of 2). The simulations have been performed in optimal condition but in reality misalignment within the column or non-ideal electrode shapes can influence the field distribution which has a direct impact on the electron beam trajectory. Therefore, the real achievable spot sizes will differ from the here determined sizes.

Estimation of the achievable ion source brightness

The second part of the simulations was performed in order to estimate the achievable ion source brightness. Ar^+ ions were generated within a cylindrical ionization volume above the ion extraction aperture, see Figure 4a. In X-direction a uniform distribution of the ion starting locations has been used whereas in the YZ-cross planes a 2D-Gaussian distribution was applied corresponding to the electron beam focusing result at 1 keV. The initial kinetic energy distribution was set to a Maxwell-Boltzmann distribution of gas temperature T = 298.15 K.

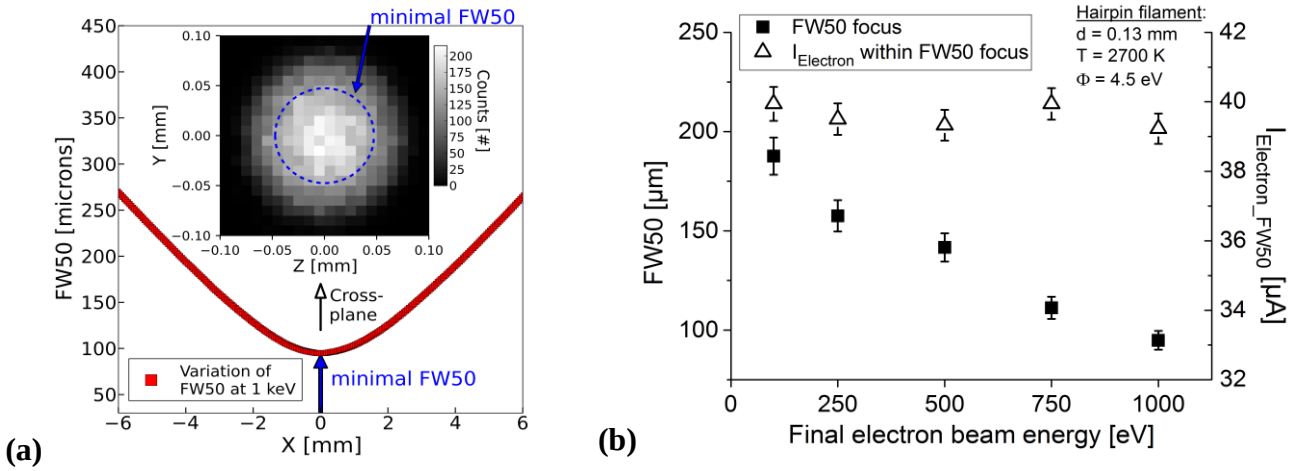

Figure 3. Simulation of the electron column: (a) FW50-variation in X-direction and 2D-histogram of the focus YZ-beam pattern at 1 keV; (b) FW50-current / -focus size depending on the final beam energy.

https://doi.org/10.1017/S1431927615013203 Published online by Cambridge University Press

In the region of the ionization volume a hard sphere collision model was applied to account for ion gas atom collisions. Inside this region the pressure p was assumed to be uniform. The total ion current generated inside the ionization volume can be calculated as follows:

$$I_{Ion\_Total} = n_{Gas}\ \sigma_{EI}\ L\ I_{Electron} \quad (2)$$

Where n_{Gas} represents the gas particle number density and σ_{EI} is the energy dependent electron impact ionization cross section (Ar^+ at 1 keV: $7.83 \cdot 10^{-21}$ m^2 [12]). L is the length of the ionization volume and $I_{Electron}$ the impinging electron beam current. The extracted ion current $I_{Ion\_Extracted}$ was determined several times for various pressures p in order to get a valid statistical representation. The results in Figure 4b represent mean values for $I_{Ion\_Extracted}$. What needs to be mentioned here is that Eq. (2) is valid only if the single collision condition is fulfilled: $n_{Gas}\ \sigma_{EI}\ L << 1$ [13]. The achievable reduced brightness B_r (current density into solid angle unit divided by beam acceleration potential) was determined by assuming that a source size (taken as FW50) d_{Source_FW50} of 10 µm and a half-opening angle α of 0.1° can be obtained for the extracted ion beam. This value of α was chosen as being a realistic target after performing a few brief ion beam simulations. The source area was taken as $A = \pi \cdot (d_{Source\_FW50}/2)^2$ and the solid angle as $\Omega = 2\pi\ (1 - \cos\alpha)$. The extracted ion beam passes further downstream through a ground aperture (not shown in Figure 4a) and the beam energy was 6 keV. Furthermore, the total electron beam current was chosen to be 50 µA. This value is less than the one determined for the electron column but reflects the fact that in reality losses will occur, e.g. due to electrode misalignment. The results can be seen in Figure 4b. An increase in extracted ion current and therefore an increase in B_r occurs with rising gas cell pressure p. For d_{Extr} = 100 µm, ΔV_{Plates} = 10 V and d_{Plates} = 1 mm the estimated B_r is 3×10^3 A m^{-2} sr^{-1} V^{-1} with an ion beam total current of 30 nA at 0.1 mbar. Gas cell pressures approaching 1 mbar result in a further increase of B_r but in that region the single collision condition loses validity and the use of equation 2 is not justified anymore. Furthermore, in reality gas conductance through d_{Extr} will be present and lead to ion gas collisions in downstream direction. This can have a negative effect on the angular confinement of the ion beam and gains more weight at higher pressures inside the gas cell.

In order to determine if the above made assumption for d_{Source_FW50} and α can be met, a first ion column optimisation has been performed by varying various parameters, e.g. electrode distances, aperture sizes or potentials. The pressure inside the ionization cell was fixed to 0.1 mbar. Likewise as for the electron column, trajectory extrapolation from a field free region beyond the ground aperture was used to find for each parameter set the corresponding d_{Source_FW50} defined as the minimal FW50 along the ion column. Moreover, at the distance D_Y of 1 m from the location of d_{Source_FW50} the FW50 was determined in the corresponding cross-beam plane (d_{FW50_1}). By calculating the size difference $\Delta d = d_{FW50\_1} - d_{VS\_FW50}$, the half-opening angle α was taken as $\alpha = \arctan(\Delta d / D_Y)$. The results for Ar^+ can be seen in Figure 5. For all shown parameter sets d_{Extr} was fixed to 100 µm. The setup of the ion column is identical for parameter set 1 and 2 with an ionization volume YZ-diameter d_{IV} of about 100 µm. The only exception is that the acceleration plate aperture diameter d_{Acc} (see Figure 4a) is smaller in the case of set 1 than for set 2. The result for set 1 shows on one hand a value of d_{Source_FW50} close to the assumption of 10 µm on the other hand α is 5 times larger compared to the assumed value. In contrast to parameter set 1, set 2 shows an α-value closer to the assumption but in this case the source size approaches 40 µm. For both sets 1 and 2, the ion-beam contains about 27 nA and has a reduced brightness of $B_r \approx 50$ A m^{-2} sr^{-1} V^{-1}. This result is clearly below the previously estimated value of $B_r = 3 \times 10^3$ A m^{-2} sr^{-1} V^{-1} at p = 0.1 mbar. For both sets d_{Source_FW50} represents a real cross-over located at a distance of a few mm away from d_{Extr} in downstream direction. In order to investigate the influence of a reduced size of the ionization volume

https://doi.org/10.1017/S1431927615013203 Published online by Cambridge University Press

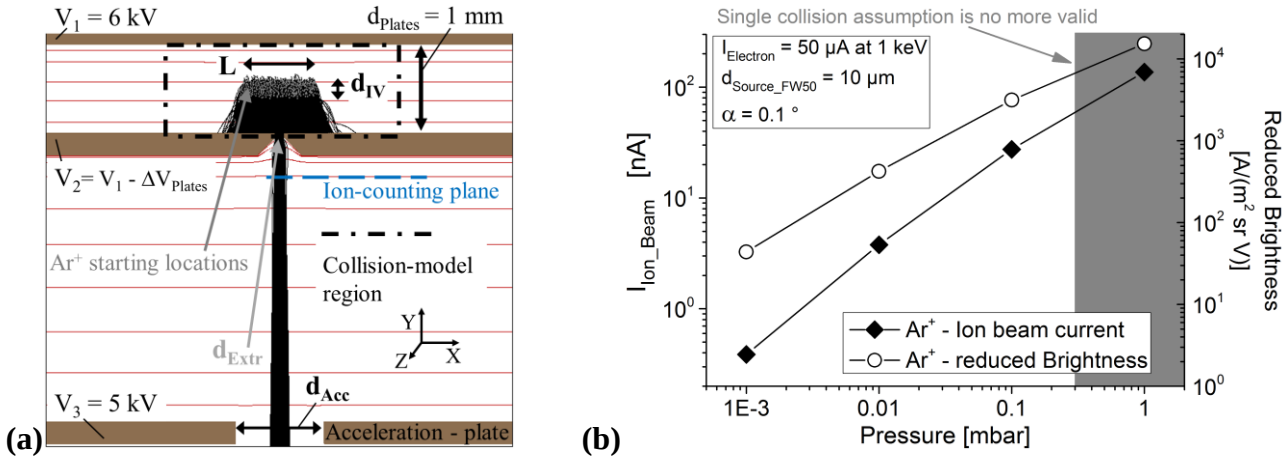

Figure 4. (a) Ion extraction simulation for Ar^+ (T = 298.15 K, p = 0.1 mbar, ΔV_{Plates} = 10 V, d_{Extr} = 100 µm); (b) ion beam current and estimated reduced brightness in dependence of the gas cell pressure p.

for set 2b the ion column setting is identical to parameter set 2, but the ionization volume YZ-diameter d_{IV} is 10 times smaller than for set 2. It can be seen that no strong change in α appears but d_{Source_FW50} is reduced and the extracted ion beam current is slightly increased as more ions are localised right above the extraction aperture. Compared to set 2, B_r is increased by a factor of 1.7. The extracted ion beam shows a higher density closer to the ion beam axis than further away. Approximately 60% of the ions pass within a disc of ≈ 80 µm in diameter concentric with the ion beam axis. By using an additional aperture it is possible to cut out the outer particle trajectories. Therefore, for parameter set 2c the ionization volume was reset to its original size with d_{IV} of about 100 µm and a beam cutting aperture of 20 µm was inserted 1 mm below d_{Extr}. Figure 5 shows that α can be clearly reduced below the assumed value of 0.1° but cutting the beam results in a slight increase of d_{Source_FW50} and a clear drop in ion beam current. Overall by comparing parameter set 2c to set 2, B_r is increased by a factor of 2.3. The last parameter set 2d shown in Figure 5 is a combination of a reduced ionization volume size combined with the use of the beam cutting aperture. In this case B_r can be increased by a factor of 6.3 compared to set 2 and reaches a value of 300 A m^{-2} sr^{-1} V^{-1}. What should be mentioned as well for the parameter sets 2b, 2c and 2d is that d_{Source_FW50} represents again a real cross-over within the first 30 mm of the ion column.

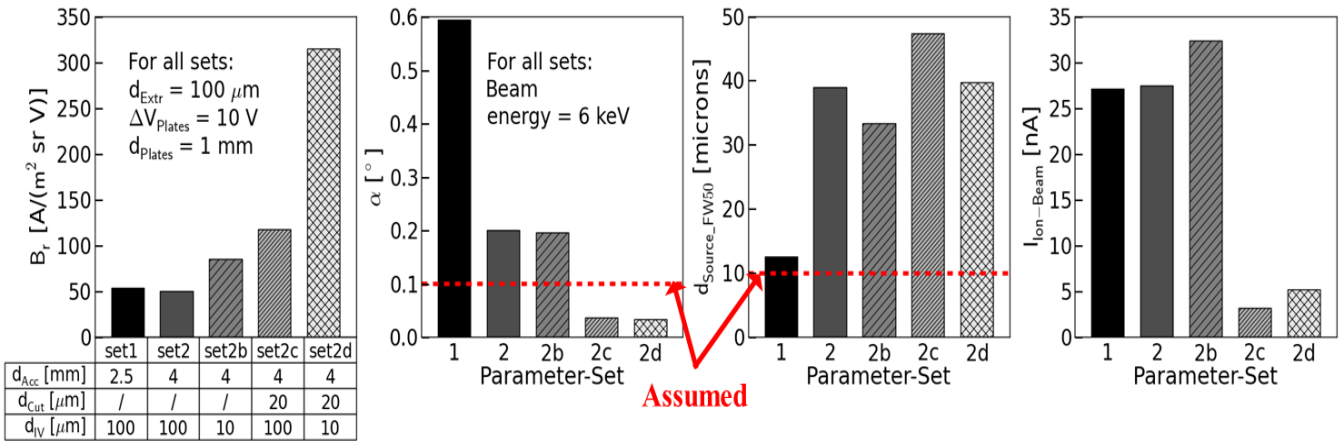

Figure 5. Chosen parameter sets to represent the results of the performed ion column optimisation (Ar^+, p = 0.1 mbar, T = 298.15 K, ΔV_{Plates} = 10 V, d_{Plates} = 1 mm, d_{Extr} = 100 µm).

https://doi.org/10.1017/S1431927615013203 Published online by Cambridge University Press

Conclusions

The electron column simulations have shown that by using a tungsten hairpin filament cathode it was possible to focus the electron beam to about 100 µm, containing a few tens of µA of current at 1 keV. The use of a single crystal LaB_6-cathode with a smaller effective emission area but comparable emitted current should lead to a better beam focus and improve the ion source performance. However, a better vacuum level compared to the filament would be required. Gas conductance calculations have shown that the actual design can reach a differential pumping capability of three orders of magnitude which would be insufficient for using an LaB_6 and a gas cell pressure of p = 0.1 mbar. A reconsideration of the column design is therefore inevitable when "upgrading" to a LaB_6 is targeted. The estimated achievable reduced ion source brightness is $B_r \approx 3\times10^3$ A m^{-2} sr^{-1} V^{-1} using p = 0.1 mbar and assuming that the ion beam has a FW50 source size of 10 µm, a half-opening angle α of 0.1° and about 30 nA of ion current. Reaching these targets would mean that the new EI-source is in terms of source size and brightness comparable to plasma sources often used for SIMS-applications [14]. A first ion column optimisation has shown that there is always a trade-off between FW50 source size and α of the ion beam. So far for a cylindrical ionization volume of a diameter d_{IV} of about 100 µm, d_{Source_FW50} is in the range of 10 to 50 µm and α between 0.2° and 0.6°. The estimated ion beam current is close to 30 nA at p = 0.1 mbar and the determined B_r is a few tens of A m^{-2} sr^{-1} V^{-1}. This represents still a clear performance improvement compared to conventional Nier type sources for which typically B_r = 1 A m^{-2} sr^{-1} V^{-1}. Moreover, by reducing the ionization volume in size or by using an ion beam cutting aperture a further improvement can be obtained leading so far at the best to $B_r \approx 300$ A m^{-2} sr^{-1} V^{-1}. Performing further ion column optimisation steps are estimated to lead to a reduced brightness approaching 1×10^3A m^{-2} sr^{-1} V^{-1}. What has to be kept in mind is that in reality a first physical effect decreasing the performance is ion scattering with residual gas atoms in downstream direction. So far a collision model is only applied in the ionization volume region, see Figure 4a. The technical setup needs to be designed so that the gas pressure beyond d_{Extr} is kept sufficiently low to minimize a spread of the extracted ion beam due to gas collisions. Secondly, space charge effects can decrease the brightness and can occur within the ionization volume region where the extraction field is only of a few V/mm. Those effects are not included in the simulations yet; doing so would enhance the reliability of the B_r - estimation, [15].

References:

[1] "Introduction to Focused Ion Beams", ed. LA Giannuzzi and FA Stevie, (Springer, New York).
[2] AA Tseng, Small **1** (2005), p. 924.
[3] LA Giannuzzi and FA Stevie, Micron **30** (1999), p. 197.
[4] NP Economou *et al*, Scanning **34** (2012), p. 83.
[5] HN Migeon *et al*, Int. J. Mass Spectrom. Ion Processes, **143** (1995), p. 51.
[6] VN Tondare, J. Vac. Sci. Technol. A **23** (2005), p. 1498.
[7] AO Nier, Rev. Sci. Instrum. **18** (1947), p. 398.
[8] JE Barth *et al*, Microelectronic Eng. **3** (1985), p. 147.
[9] SIMION 3D version 8.1; Scientific Instrument. Services, Inc.
[10] D Dowsett, this proceedings.
[11] S Yamamoto, Rep. Prog. Phys. **69** (2006), p. 181.
[12] R Rejoub *et al*, Phys. Rev. A **65** (2002), 042713.
[13] TD Märk in "Electron Ionization", ed. TD Märk and GH Dunn, (Innsbruck Uni. Press) p. 137.
[14] NS Smith *et al*, Appl. Surf. Sci. **255** (2008), p. 1606.
[15] This work is supported by the Fonds National de la Recherche, Luxembourg (AFR-Grant 5944057)

https://doi.org/10.1017/S1431927615013203 Published online by Cambridge University Press